Available online at www.sciencedirect.com
ScienceDirect
Journal of Nuclear Materials 357 (2006) 169–182
journal of nuclear materials
www.elsevier.com/locate/jnucmat

Mechanical properties of neutron-irradiated nickel-containing martensitic steels: II. Review and analysis of helium-effects studies

R.L. Klueh [a,*], N. Hashimoto [a], M.A. Sokolov [a], P.J. Maziasz [a], K. Shiba [b], S. Jitsukawa [b]

[a] *Oak Ridge National Laboratory, Metals and Ceramics Division, Building 4500S, P.O. Box 2008, MS 6151, Oak Ridge, TN 37831-6151, USA*
[b] *Japan Atomic Energy Research Institute, Tokai-mura, Naka-gun, Tokai, Ibaraki 319-1195, Japan*

Received 14 November 2005; accepted 17 May 2006

Abstract

In part I of this helium-effects study on ferritic/martensitic steels, results were presented on tensile and Charpy impact properties of 9Cr–1MoVNb (modified 9Cr–1Mo) and 12Cr–1MoVW (Sandvik HT9) steels and these steels containing 2% Ni after irradiation in the High Flux Isotope Reactor (HFIR) to 10–12 dpa at 300 and 400 °C and in the Fast Flux Test Facility (FFTF) to 15 dpa at 393 °C. The results indicated that helium caused an increment of hardening above irradiation hardening produced in the absence of helium. In addition to helium-effects studies on ferritic/martensitic steels using nickel doping, studies have also been conducted over the years using boron doping, ion implantation, and spallation neutron sources. In these previous investigations, observations of hardening and embrittlement were made that were attributed to helium. In this paper, the new results and those from previous helium-effects studies are reviewed and analyzed.

1. Introduction

Without a fusion test reactor or other intense 14 MeV neutron source, simulation techniques are required to study the possible effects of neutron irradiation from the deuterium–tritium fusion reaction that will cause the simultaneous production of displacement damage and transmutation helium in a martensitic steel first wall of a fusion reactor. In part I of this work, results from the irradiation of modified 9Cr–1Mo (9Cr–1MoVNb), Sandvik HT9 (12Cr–1MoVW),[1] and these steels with 2% Ni (9Cr–1MoVNb–2Ni and 12Cr–1MoVW–2Ni) in the High Flux Isotope Reactor (HFIR) and the Fast Flux Test Facility (FFTF) were presented [1]. Tensile results indicated helium-induced hardening

* Corresponding author. Tel.: +1 865 574 5111; fax: +1 865 241 3650.
E-mail address: kluehrl@ornl.gov (R.L. Klueh).

[1] The commercial steels modified 9Cr–1Mo and Sandvik HT9 will be referred to by the generic designations 9Cr–1MoVNb and 12Cr–1MoVW, respectively.

0022-3115/$ - see front matter © 2006 Elsevier B.V. All rights reserved.
doi:10.1016/j.jnucmat.2006.05.049

caused an increase in the ductile–brittle transition temperature (DBTT) above that caused by displacement damage and irradiation-induced precipitation effects occurring in the absence of helium. Previous work on the nickel-doped steels irradiated to a much higher dose [2–6] indicated helium caused embrittlement, but without detectable hardening above that attributed to displacement damage and irradiation-induced precipitation [5,6].

In this paper, results from these helium-effects studies using nickel doping and other simulation techniques are reviewed and analyzed. The objective is to place the recent results [1] in context with previous studies to demonstrate the effect of helium on mechanical properties of irradiated ferritic/martensitic steels.

2. Experimental techniques

Several techniques have been used to study helium effects, including nickel doping [1–7], boron doping [8,9], helium implantation with accelerators [10–14] and injector foils [15–17], and spallation neutron sources [18–25]. All but the injector foils have been employed for mechanical properties studies, which are the subject of this paper. In this section, the techniques used to study mechanical properties will be briefly described.

2.1. Nickel doping

Simultaneous displacement damage and helium formation is produced in alloys containing nickel irradiated in a mixed-spectrum fission reactor. Displacement damage is produced by fast neutrons in the spectrum, and helium forms by a two-step reaction of ^{58}Ni with thermal neutrons in the spectrum [7]: ^{58}Ni(n,γ)^{59}Ni(n,α)^{56}Fe (natural nickel contains 68% ^{58}Ni). For ferritic/martensitic steels with about 2% Ni, irradiation in a mixed-spectrum reactor such as HFIR at the Oak Ridge National Laboratory (ORNL) produces a similar helium to displacement damage ratio ($\approx$10 appm/dpa) to that attained in a tokamak first wall in the steel without the nickel when irradiated to $\gtrsim$10 dpa. Atom recoil resulting from the (n,α) reaction produces displacement damage in the metal lattice that needs to be accounted for [26].

As part I of this work, tensile and Charpy results were published for 9Cr–1MoVNb and 12Cr–1MoVW steels and these steels with 2% Ni that were irradiated to 12 dpa at 400 °C in HFIR and to 15 dpa at 393 °C in the FFTF [1]. The technique was also used in earlier experiments for irradiation of the steels up to $\approx$40 dpa at 400 °C in HFIR and FFTF [2–6]. To determine whether there is a helium effect, tensile and Charpy data for steels with and without nickel additions were compared after irradiation in HFIR, and data for steels irradiated in HFIR were compared with those irradiated in FFTF, where very little helium is produced.

Uncertainties in the nickel-doping technique involve the possible effect of nickel on the microstructure. Irradiations of nickel-containing 9Cr steels to low doses in the Japan Materials Test Reactor (JMTR) [27] and the Advanced Test Reactor (ATR) [28] at temperatures below 300 °C indicated an effect of nickel on hardening. As discussed in detail in part I [1], no such hardening has been observed for irradiations at 300 and 400 °C in HFIR and at 393 °C in FFTF, which are the focus of this discussion.

2.2. Boron doping

Boron-containing steels have been used to study helium effects [8,9,29–33], because during neutron irradiation, helium forms by the ^{10}B (n,α)^{7}Li reaction. The cross section for the (n,α) reaction is greatest for low-energy (thermal) neutrons, which means irradiation in a mixed-spectrum reactor such as HFIR will cause all the ^{10}B to transform within 1–2 dpa, compared to a much longer time in a fast reactor. Natural boron contains about 19.9% ^{10}B, the remainder ^{11}B.

The energies of the lithium ion and the α-particle (0.87 and 1.53 MeV, respectively) produced by the reaction create a significant number of atomic displacements as they slow down to thermal energy, and these additional displacements could cause an increase in the local defect concentration [34]. Boron can segregate to interfaces and form precipitates or be incorporated in precipitates, such as B_4C and $M_{23}(CB)_6$ [35,36]. When the boron is contained in precipitates, neutron irradiation can lead to cavities forming in a 'halo' around the boron-containing precipitate particles, the size of the halos being characteristic of the energy of the α-particles released by the (n,α) reaction. Sometimes two rings are observed, one for the α-particle and one for the lithium [35,36]. The presence of the lithium could present a source of confusion in the interpretation of the results.

2.3. Helium implantation

Helium can be implanted in miniature tensile or Charpy specimens by α-particle injection in a cyclotron [10–14]. An injected specimen can then be compared to a similar specimen irradiated by neutrons in a reactor to a similar dose, but where much less helium is formed. Alternatively, the implanted specimen can be compared with an unimplanted specimen [11–14]. A problem with this technique is that it produces a higher He/dpa ratio than fusion, and it is generally limited to low doses.

2.4. Spallation neutron source irradiation

Obviously, nickel doping, boron doping, and helium implantation experiments are not ideal for simulating helium effects for fusion applications. An ideal experiment would produce helium during irradiation without altering the steel composition, as in a fusion reactor or an intense 14 MeV neutron source. Although different from fusion conditions, high-energy proton or neutron irradiation in spallation neutron sources have been used to investigate simultaneous production of helium and displacement damage without introducing another element or implanting helium [18–25]. In such facilities, irradiation is by very high-energy particles, much higher than the 14 MeV neutrons emanating from the deuterium–tritium fusion reaction.

Most of the studies discussed below were carried out on ferritic/martensitic steels irradiated by 600–750 MeV protons in SINQ (Swiss Spallation Neutron Source) at the Paul Scherrer Institute in Switzerland [18–22]. Studies have also been carried out in the LANSCE (Los Alamos Neutron Science Center) accelerator at Los Alamos, New Mexico [23–25].

Problems with spallation neutron irradiation include a much higher He/dpa ratio compared to that for an intense 14 MeV neutron source, and in addition to helium, large amounts of hydrogen are also produced.

3. Review of experimental results

All four experimental techniques introduced in the previous section have produced results that were interpreted to indicate a helium effect on swelling and embrittlement of ferritic/martensitic steels. In this section, similarities and differences in these results will be summarized and discussed.

3.1. Nickel doping

Nickel doping has been used to examine the effect of helium on swelling [37,38] and tensile [1–4] and impact properties [1,5,6,39] of ferritic/martensitic steels by comparing the effects when irradiated in the mixed-spectrum HFIR reactor and the FFTF fast reactor. Although an increase in swelling has been attributed to the higher helium generated in HFIR when nickel-doped steels irradiated in the HFIR and FFTF reactors were compared, there was no apparent difference in precipitation during irradiation [37,38]. Precipitates in the 9Cr–1MoVNb and 12Cr–1MoVW steel with and without the nickel additions were examined by transmission electron microscopy (TEM) after irradiation at 407 °C to ≈47 dpa in FFTF and at 400 °C to ≈38 dpa in HFIR [37,38]. The same high density of tiny M_6C precipitates formed in 9Cr–1MoVNb–2Ni and 12Cr–1MoVW–2Ni during irradiation in FFTF as formed in HFIR.

In the most recent experiment with nickel-doped steels to examine the effect of helium on mechanical properties, 9Cr–1MoVNb, 9Cr–1MoVNb–2Ni, 12Cr–1MoVW, and 12Cr–1MoVW–2Ni steels were irradiated in HFIR to ≈10 dpa at 300 °C and ≈12 dpa at 400 °C and to ≈15 dpa at 393 °C in the FFTF [1]. The results indicated that the 9Cr–1MoVNb–2Ni (129 appm He), 12Cr–1MoVW (31 appm He), and 12Cr–1MoVW–2Ni (141 appm He) irradiated in HFIR hardened more – showed a larger increase in yield stress, $\Delta\sigma_y$ – than the same steels irradiated in FFTF at 393 °C (<0.5 appm He). The 9Cr–1MoVNb steel, which contained the least helium (12 appm), hardened to about the same level in both FFTF and HFIR. These results along with the 300 °C results from HFIR for the steels with and without the nickel additions led to the conclusion that helium caused a larger $\Delta\sigma_y$ than that due to displacement damage and any irradiation-induced precipitation hardening [1].

The increment of hardening contributed to an increase in DBTT (ΔDBTT) over and above that when there was no helium present. Irradiation in HFIR at 300 and 400 °C caused a larger ΔDBTT for the steels containing 2% Ni than for those with no nickel addition. There was a linear relationship between ΔDBBT and $\Delta\sigma_y$, and the data were fit by linear regression through the origin. Since there were no FFTF irradiations for comparison for the 300 °C HFIR irradiations, this discussion will emphasize the 400 °C HFIR data and the 393 °C

FFTF data, for which the slope of the ΔDBTT–$\Delta\sigma_y$ relationship was 0.42 [1].

In the previous paper, these data for the 10–15 dpa HFIR and FFTF irradiations were compared with previous 40 dpa irradiations in HFIR [5] at 400 °C and high-dose irradiations in EBR-II at 390 °C [40]. The high-dose results also provided indications of a helium effect on fracture, because there was a much larger ΔDBTT for the HFIR-irradiated specimens compared to the EBR-II-irradiated specimens and a larger ΔDBTT for the nickel-doped specimens compared to the undoped specimens irradiated in HFIR .

There were some differences between the high-dose and low-dose irradiations. First, fracture of the nickel-doped specimens from the high-dose irradiations displayed an intergranular fracture mode on the lower shelf [5], compared to transgranular cleavage for the low-dose irradiations [1]. Secondly, the data for the high-dose HFIR experiment (HFIR #1) [5] did not fit on the linear ΔDBTT–$\Delta\sigma_y$ relationship (Fig. 1) obtained from the recent HFIR experiment (HFIR #2) [1]. Fig. 1 indicates a much larger ΔDBTT for the high-dose data than would be predicted from the linear relationship based on the low-dose data. It appears that softening occurred for the high-dose specimens compared to the linear relationship of the low-dose specimens. For the combined data for the two studies, there appeared to be a relationship between ΔDBTT and helium concentration [1].

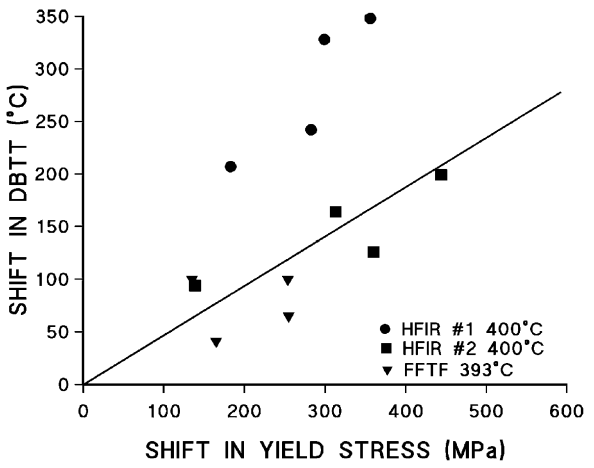

Fig. 1. Shift in ductile–brittle transition temperature plotted against the increase in yield stress for 9Cr–1MoVNb, 9Cr–1MoVNb–2Ni, 12Cr–1MoVW, and 12Cr–1MoVW–2Ni steels irradiated in the present (HFIR #2) and previous (HFIR #1) HFIR experiments at 400 °C and in FFTF at 393 °C.

3.2. Boron doping

The effect of helium on swelling was investigated in the reduced-activation steel F82H (nominally Fe–2.0W–0.20V–0.04Ta–0.10C) with 4–8 and 60 ppm natural boron (≈6 and 60 appm He) and 58 ppm ^{10}B (≈300 appm He). Irradiation at 400 °C in HFIR to ≈7, 26, and 51 dpa [41] demonstrated that swelling and the number density of cavities increased with helium concentration.

Tensile specimens of the reduced-activation steel F82H with the above boron concentrations were irradiated in HFIR at 400 and 500 °C to 11–34 dpa [8,9]. Tests at the irradiation temperatures indicated that any effect of helium on strength or ductility was small, and the differences generally fell within the scatter of the data. These steels were also irradiated in the Japan Materials Test Reactor (JMTR) to 0.8 dpa at 250–265 °C [8,9]. For tensile tests over the range from room temperature to 400 °C, irradiation hardening for the two steels was similar, with boron-doped F82H showing a slightly lower strength. However, the steel with the higher helium concentration had a considerably lower total elongation and reduction of area [9].

Several irradiation experiments indicated that specimens with 300 appm He from ^{10}B had a much larger ΔDBTT than specimens without the presence of helium or with much lower helium concentrations [8,9,29–33]. Irradiation of ^{10}B-doped specimens and undoped specimens at 355–375 °C to 0.3–0.5 dpa in JMTR and the Japan Research Reactor (JRR-2) to produce 300 appm He in the doped F82H produced a DBTT in the doped steel ≈15 °C higher than in the undoped steel [8]. No shift in transition temperature was observed when irradiated at 500–590 °C.

A larger effect with ^{10}B doping was obtained for F82H irradiated at lower temperatures (260–360 °C) to 0.3–0.6 dpa in JMTR [9]. Although a complete Charpy curve was not determined (because of temperature limitations of the Charpy test rig) for the ^{10}B-doped steel with 100 appm He, the ΔDBTT appeared to be well above room temperature (Fig. 2) and much larger than for the standard F82H irradiated similarly. There was no difference in the yield stress of the ^{10}B-containing steel and a steel without the ^{10}B addition. Both hardened by a similar amount, although there was a slight loss of ductility for the ^{10}B-containing steel [9].

In another experiment, the reduced-activation steel JLF-1 (nominally Fe–9Cr–2.0W–0.20V–0.07Ta–0.05N–0.10C) and this steel with 0.0022%

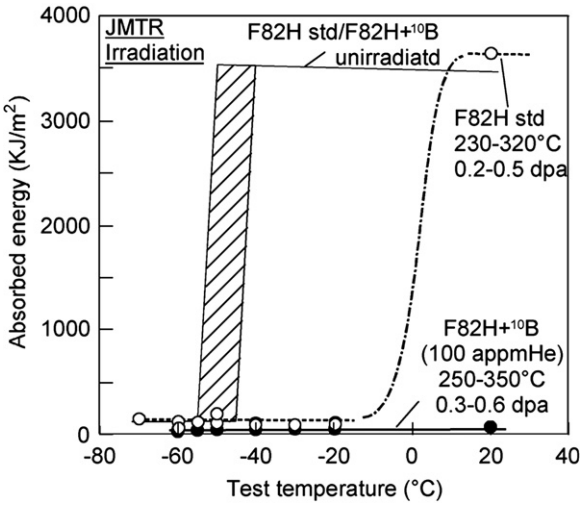

Fig. 2. Charpy impact curves for standard F82H and ^{10}B-doped F82H in the unirradiated condition and after irradiation to 0.2–0.6 dpa at 250–350 °C in JMTR [9].

B was irradiated to 2.5 dpa at 300 °C in the High Flux Reactor (HFR), a mixed-spectrum reactor in the Netherlands [29]. Before irradiation, the steels had similar Charpy curves. After irradiation, the DBTT of the boron-containing steel with ≈23 appm He was about 70 °C higher than for the steel without the boron addition.

The relative shift in DBTT obtained from irradiation in HFR of four reduced-activation steels and two conventional Cr–Mo steels after 0.2, 0.8 and 2.4 dpa at 250–450 °C was attributed to the different levels of helium in the steels due to different levels of boron [30–32]. In Fig. 3, the ΔDBTT data for these steels are shown as a function of dose for the 300 °C irradiation along with the boron content of each steel. It was observed that the higher the boron content, the steeper the slope of the curve and the higher the ΔDBTT for the individual steels. A curve for the ^{10}B-to-He transformation is also shown, and it has the same characteristics as the embrittlement curves. Over 99% of the ^{10}B has transformed to helium by 1.6 dpa, which is near where saturation in ΔDBTT with fluence occurred for the MANET I steel.

Maximum helium in the steels was calculated as 85, 70, 60, 60, <20, and <10 appm for MANET I, MANET II, OPTIFER Ia, OPTIFER II, F82H, and ORNL 9Cr–2WVTa, respectively. The ΔDBTTs for the steels scale with the boron content and, therefore, the helium content; the ratio of ΔDBTT to helium was essentially the same for all of the steels at ≈2–3 °C/appm He [30–32]. The effect of helium (boron) was subsequently 'verified' by irradiating OPTIFER steels with reduced boron concentrations [33]. These steels showed significantly less embrittlement than the same steels containing the higher boron concentrations.

3.3. Helium implantation

To investigate the effect of helium on embrittlement, 300 appm He (0.2 dpa) was implanted in miniature Charpy specimens of F82H by α-particle injection in a cyclotron [10]. For comparison, similar specimens were irradiated in the HFR to the same dose but with <8 appm He. The ΔDBTT of the latter specimen was 18 °C compared to 44 °C for the implanted specimen. The results were interpreted to mean helium exacerbated the shift in DBTT [10].

In a another study, up to 5000 appm He was implanted at 150–550 °C in 100 μm thick tensile specimens of normalized-and-tempered modified 9Cr–1Mo (9Cr–1MoVNb) and EM10 (Fe–8.8Cr–1.1Mo–0.5Mn–0.2Ni–0.4Si–0.1C that is essentially unmodified 9Cr–1Mo steel) [11]. Tests at room temperature and the implantation temperature indicated that implanted helium caused hardening and embrittlement, which increased with increasing helium and decreasing implantation temperature. For steels containing about 2500 appm He, scanning electron microscopy (SEM) revealed intergranular failures. For irradiation at 250 °C and testing at either room temperature or 250 °C, failure occurred with little or no necking, and the fracture surface was essentially completely intergranular. It was stated that tests on steel irradiated at 550 °C, 'displayed some necking and ductile appearance is retained . . .' [11].

In more recent work, these investigators implanted 2500 appm He in miniature tensile specimens and the notch region of Charpy specimens at 250 °C with a displacement damage of 0.4 dpa [13,14]. Room-temperature 0.2% yield stress increased by ≈50% after implantation, with an accompanying decrease in ductility; total elongation decreased from about 9% to about 1%. Although SEM of fracture surfaces indicated a ductile failure, there were indications of secondary cracks on grain boundaries. Charpy specimens were tested in static three-point bending at room temperature. Bending curves indicated a 'pop-in' in a narrow loading range, indicating the initiation and propagation of

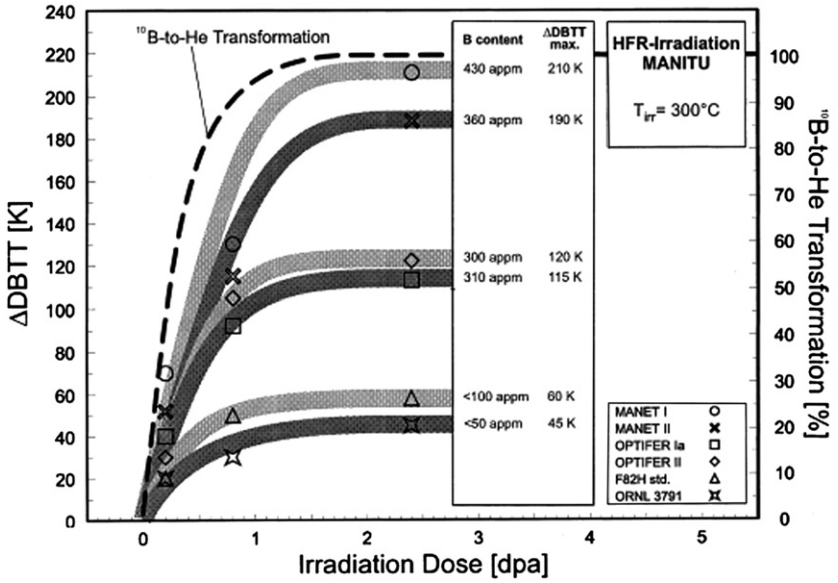

Fig. 3. Shift in DBTT vs. irradiation dose of six steels irradiated in HFR showing how the shift in DBTT correlates with boron content, and therefore, helium content [30].

a brittle crack. A fully brittle fracture containing intergranular and cleavage fracture modes was observed by SEM in the helium-implanted region, whereas a ductile failure mode was observed in the non-implanted region. Finite-element analysis of the bending tests demonstrated that helium caused a decrease in the critical stress for intergranular fracture [13].

The TEM observations on EM10 and modified 9Cr–1Mo (identified in the studies as T91 – the ASTM designation for modified 9Cr–1Mo tubing) specimens irradiated at 250 and 550 °C with 5000 appm He showed high number densities of helium bubbles, similar in appearance for both steels [12]. The helium bubbles in specimens irradiated at 250 °C were too small to detect by TEM, but black-dot damage was observed. Small-angle scattering verified the presence of bubbles in these specimens. Bubbles were observed by TEM in specimens irradiated at 550 °C. They were estimated at 2.5–3 nm in diameter at a number density of $3–4 \times 10^{22}$ m^{-3}; they were inhomogeneously distributed in the matrix, on lath boundaries and prior-austenite grain boundaries, on dislocations, and at carbide/matrix interfaces. It was concluded that the bubble pressures were close to thermodynamic equilibrium, and hardening was due to the high density of helium bubbles that leads to the intergranular fracture, and the [12], 'brittle, intergranular fracture mode results from the combination of pronounced hardening and weakening of PAG [prior-austenite grain] boundaries due to helium'. In the second experiment where implantation was to 2500 appm at 250 °C, the number density of small (<1 nm) bubbles was estimated at $3–4 \times 10^{23}$ m^{-3} [14].

It is interesting to note that since the objective of these tests was the determination of the feasibility of using martensitic steels for the target of a European Spallation Source (ESS), the results were taken as putting into question [12], '... the suitability of martensitic steels as structural materials for the ESS container window, which will operate below 250 °C'. Applications at temperatures significantly higher than 250 °C were deemed possible.

3.4. Spallation neutron source irradiation

Studies on microstructure [18,21,22], tensile properties, and impact properties [18–22] were conducted on several martensitic steels after irradiation by 600–750 MeV protons in SINQ. Most of the observations were on T91 (9Cr–1MoVNb) and F82H. Two SINQ irradiations were carried out, one to doses up to 12 dpa and 1120 appm He at 90–360 °C and the other up to 20.3 dpa and 1695 appm He at 118–400 °C [18–22].

Helium bubbles 1–1.5 nm diameter formed in the steels irradiated at 175–360 °C up to ≈12 dpa and

1100 appm He; there a slight increase in size with irradiation temperature. Number density remained relatively constant over the temperature range at $\approx 5 \times 10^{23}$ m^{-3}. No bubbles could be resolved for irradiations below about 5.8 dpa, indicating helium concentration was not high enough [18,22].

In the second experiment on F82H irradiated at 400 °C to 20.3 dpa and 1695 appm He, a bimodal distribution of bubbles and/or voids was observed. The size of the cavities reached 60 nm, thus indicating the large effect of helium and temperature [22] relative to studies in the first experiments at lower temperatures and doses [18,22].

Tensile tests on steels irradiated at 90–360 °C up to 12 dpa indicated hardening increased with dose. Sufficient specimens were not available to determine whether saturation in strength occurred with increasing dose [19,22].

Small-punch (SP) testing was used to determine a $DBTT_{SP}$ [19,21,22], as differentiated from Charpy V-notch (CVN) tests, which were also conducted to determine $DBTT_{CVN}$ [22]. The $\Delta DBTT_{SP}$ increased linearly with dose up to 6–7 dpa and about 400 appm He, above which there was a large increase for both F82H and T91. There was no saturation of $\Delta DBTT_{SP}$ with dose. Based on the determined relationship $DBTT_{SP} = 0.4\ DBTT_{CVN}$, a shift of $DBTT_{CVN}$ of 295 °C was calculated for T91 irradiated to 9.4 dpa at 280 °C. A linear relationship between $\Delta DBTT_{SP}$ and helium concentration was observed [22], similar to that obtained for the nickel-doping experiments [1].

A limited number of tests on CVN specimens of T91 and F82H irradiated to 7.5 dpa at 120–195 °C also showed the non-linear increase with dose indicated in the SP tests. These tests verified the relationship between $DBTT_{SP}$ and $DBTT_{CVN}$ [21]. There was no indication of a saturation with dose.

In the second, higher-dose experiment, SP specimens of F82H were irradiated up to 18.4 dpa and ≈1530 appm He at an average temperature of 380 °C. The $\Delta DBTT_{SP}$ was 291 °C, which gives a calculated $\Delta DBTT_{CVN}$ of 727 °C. These results combined with the other results reinforced the conclusions that ΔDBTT does not saturate with dose, and there is a linear relationship between ΔDBTT and helium concentration for the steels irradiated over the range 2.5–18.4 dpa and 85–1530 appm He [22]. With SEM observations on tested small-punch specimens, it was possible to observe the change in fracture mode from brittle to ductile with increasing test temperature. Brittle fracture appeared to be highly intergranular.

Evidence that helium can promote intergranular fracture was obtained in a related experiment in SINQ, where tensile specimens of EM10 were irradiated in the normalized-and-tempered, quenched, and cold-worked-and-tempered conditions [42,43]. Average irradiation conditions were ≈100–330 °C, 4–12 dpa, and 150–940 appm He. The quenched steel is of interest for this discussion because after irradiation at an average temperature of 287 °C to 9.8 dpa and 750 appm He, the specimen tested at room temperature fractured without necking, and SEM indicated that [43], '... the fracture surface, which lies strictly perpendicular to the specimen axis, displays a fully brittle, intergranular appearance'. This observation contrasted with the unirradiated steel that displayed a fracture that, 'is clearly fully ductile as shown by the well defined dimples'.

Results from this irradiation in SINQ were compared with irradiation to 0.8–9 dpa at 325 °C of the same EM10 in the quenched condition in the mixed-spectrum OSIRIS Reactor [41]. Despite even greater hardening of the quenched steel irradiated in OSIRIS, it was stated that the specimen can [43] 'still retain some ductility ... whereas the SINQ-irradiated specimens display a complete loss of ductility'. Reduction of area for a room-temperature test was >50% for the OSIRIS-irradiated specimen, compared to essentially no reduction of area for the SINQ-irradiated specimen, indicating the complete embrittlement of this specimen [43].

It appears that in all attempts to study helium effects, interpretation of results is always associated with inherent uncertainties, and these experiments are no exception. Although helium is implicated in the intergranular fracture, the investigators pointed out that considerable hydrogen (over 4000 appm) was generated during the SINQ irradiation, and it could be a contributing factor [43]. However, they concluded that a substantial amount of this hydrogen should diffuse from the steel during irradiation. To support this, work was cited that showed only 10% of the hydrogen generated in F82H irradiated in SINQ at 295 °C remained in the steel following irradiation [44]. The quenched EM10 was irradiated at 287 °C. It was also pointed out that if hydrogen was the source of the intergranular failure, then a similar effect might be expected for the normalized-and-tempered and cold-worked-and-tempered steels [43]. Also, the helium-implantation study

discussed in the previous section [11,12] that gave similar intergranular fractures without the presence of hydrogen was cited to support the conclusion that intergranular fracture was caused by the helium.

Several ferritic/martensitic steel tensile specimens were irradiated in LANSCE and HFIR, including modified 9Cr–1Mo and the reduced-activation steel ORNL 9Cr–2WVTa. Irradiation was at 60–100 °C at doses up to 1.2 dpa in HFIR and 60–164 °C at doses of 0.026–10 dpa in LANSCE [24,25]. The interesting observation for this discussion is the conclusion that [25]: 'there are signs of a small radiation strengthening contribution attributable to the presence of helium'. This hardening due to helium appears similar to that observed in the low-dose irradiations of the nicked-doped steels [1].

4. Discussion

4.1. Analysis of data

In the recent irradiation experiments on nickel-doped and undoped 9Cr–1MoVNb and 12Cr–1MoVW steels irradiated to 12-15 dpa in HFIR and FFTF at ≈400 °C, the results indicated that helium increased the hardening and embrittlement over that due to displacement damage and irradiation-induced precipitation [1]. These results agreed with previous experiments at low irradiation temperatures [2,39], but they differed from previous HFIR experiments on these same steels irradiated to 40 dpa at 400 °C (Fig. 1) that led to the conclusion that helium causes embrittlement by causing a change in fracture mode [5,6].

Reasons for concluding there was a helium effect in the recent experiments were: (1) the ΔDBTTs for the HFIR-irradiated steels with the highest helium concentrations were greater than for the same steels with much less helium after irradiation in FFTF to similar doses, (2) ΔDBTTs of the HFIR-irradiated 9Cr–1MoVNb–2Ni and 12Cr–1MoVW–2Ni steels were greater than those for the steels without nickel additions, and (3) HFIR-irradiated steels with the highest helium concentrations generally hardened more than the same steels irradiated in FFTF.

A similar hardening effect due to helium was recently observed in dual-ion irradiations [45]. Specimens of reduced-activation steel JLF-1 were irradiated with single-beam 6.4 MeV Fe^{3+} ions and with the double-beam 6.4 MeV Fe^{3+} ions and 1.0 MeV He^{3+} ions at 420 °C up to 60 dpa. Dual-ion irradiation produced finer defect clusters than single-ion irradiation. Nano-indentation hardness measurements indicated much more hardening for the dual-ion irradiated specimens. Further, the hardening appeared to saturate for the single-ion-irradiated specimens, but not for the dual-ion-irradiated specimens, even after 60 dpa [45].

The ΔDBTTs in the recent work [1] were not as large as in the previous experiment on nickel-doped steels (Fig. 1) [5]. Furthermore, there appeared to be a correlation between ΔDBTT and $\Delta\sigma_y$ for the recent experiments, which is contrary to the previous high-dose experiments at 400 °C, where no hardening in 400 °C tensile tests was attributable to helium [3,4]. Also, in the recent experiments, there was no indication of intergranular fracture. As discussed below, it was previously suggested that helium can promote intergranular fracture in an impact test, and intergranular fracture was observed on nickel-containing steels irradiated to >60 dpa and up to >700 appm He [4,5].

The TEM on the 9Cr–1MoVNb–2Ni steel irradiated at 400 °C to about 12 dpa provided further support for the conclusion of a helium effect [1,46]. In this case, the high number density of small M_6C particles observed in the high-dose irradiations [37,38] was not observed. Instead, the irradiation-induced precipitate that appeared was M_2X, and it was present at a lower number density (5×10^{20} m^{-3}) and a larger size (54 nm) than the M_6C in this steel irradiated to 38–47 dpa in HFIR and FFTF. Irradiation-induced M_6C was observed in a reduced-activation 9Cr–2WVTa steel containing 2% Ni (9Cr–2WVTa–2Ni); the number density was estimated to be 2×10^{21} m^{-3} with an average size of 7 nm [1,46]. This irradiation was also to 12 dpa in HFIR at 400 °C, and the specimen was contained in the same capsule used for the 9Cr–1MoVNb–2Ni. It is of interest to note that the hardening ($\Delta\sigma_y$) in the two steels was similar (313 MPa for the 9Cr–1MoVNb–2Ni and 301 MPa for the 9Cr–2WVTa–2Ni), another indication, perhaps, that these particular irradiation-induced precipitates were not a major component of the hardening, given the large difference in size and number density of the precipitates in the two steels.

Although results from the recent experiment (to ≈12 dpa) and those from the previous experiment (to ≈40 dpa) for 400 °C irradiations in HFIR led to conclusions of a helium effect on impact properties, there appear to be different mechanisms. In the first case, excess hardening by helium appeared to

play a role [1]. In the second case, no excess hardening attributable to helium was observed. Instead, softening occurred relative to the steel irradiated to 12 dpa (Fig. 1), and helium appeared to promote intergranular failure [5].

According to Farrell [47], helium can affect the mechanical properties in three ways: (1) helium can stabilize vacancy clusters, thus causing an increase in the number of interstitial clusters that eventually grow into dislocations that increase the strength, (2) helium can stabilize the clusters to higher temperatures than in the absence of helium, and (3) helium can diffuse to grain boundaries and induce intergranular failure.

Another possible hardening mechanism for helium is a high number density of small helium-filled bubbles, such as those observed by helium implantation [11–14,48] and spallation neutron source irradiations [18,22]. There are still some question of how much hardening occurs in this instance. Modeling of the interaction of an edge dislocation with voids showed that the voids down to 1 nm are strong obstacles for dislocations [49]. However, molecular dynamic simulations indicated voids are weak barriers, and helium-filled bubbles are only moderately more effective [50].

The transition temperature in an impact test can be increased by an increase in flow stress or a decrease in fracture stress. Displacement damage and irradiation-induced precipitation can cause embrittlement by increasing the flow stress. Hardening by helium should have the same effect. Since the shift in transition temperature for the high-dose experiments was not commensurate with the hardening observed – if anything, there was a relative softening – it was hypothesized that helium lowered the fracture stress [5,6]. An increase in DBTT due to a lower fracture stress can be caused by: (1) more or larger flaws at which a fracture initiates, (2) less resistance to initiation of a flaw, and (3) less resistance to the propagation of a flaw.

Inclusions or carbides are the usual source of the microcracks that initiate fracture in steels [51,52]. To explain a helium effect for the high-dose irradiations, a mechanism was hypothesized previously [5,6] that when steels contain sufficient helium, the microcrack source could be helium-containing bubbles on a prior austenite grain boundary, on a martensite lath boundary (subgrain boundary), or at a precipitate/matrix interface. Helium could collect in small bubbles that under stress become nuclei for fracture and/or enhance crack propagation, thus providing an explanation for observations of intergranular facets on the fracture surface [5]. Helium-caused flaws could induce brittle fracture, but the fracture mode would not be completely intergranular until a high concentration of helium is present. With higher helium concentrations at boundaries, resistance to crack propagation could be affected. A change to a fully intergranular fracture would be accelerated by increased helium and higher temperatures, where diffusion rates of helium to boundaries would be higher [5,6].

Such fine bubbles on boundaries have been observed on 9Cr–1MoVNb–2Ni irradiated at 400 °C to ≈75 dpa and ≈760 appm He (Fig. 4) [53]. As seen in Fig. 4, an almost continuous layer of tiny bubbles cover the $M_{23}C_6$ particles and the lath boundaries that contain the precipitate. These fine bubbles, some of which are also visible in the matrix, are distinct from the large polyhedral cavities in the matrix. From the appearance of the bubbles lining the boundaries in Fig. 4, it is easily visualized how an applied stress could nucleate a crack.

Results from the low- and high-dose experiments indicate that helium could affect embrittlement by two of Farrell's mechanisms [47]: (1) by a hardening mechanism at low doses and (2) by promotion of intergranular fracture at high doses. Hardening by helium-filled bubbles, such as those in the matrix in Fig. 4, could also contribute to hardening and embrittlement. This contribution would be expected to contribute most when the bubbles are smaller in the low-to-intermediate helium concentration regime.

The fact that ΔDBTTs observed after 40 dpa at 400 °C [5] did not correlate with the hardening (Fig. 1) observed in the recent experiment [1] can also be explained by the difference in dose. Hardening saturates with fluence in a fast reactor after a few (<10) dpa at 400 °C. As opposed to saturation occurring for higher-dose experiments in fast reactors (low helium), however, a maximum in yield strength and transition temperature with fluence has been observed for several steels [54–58], including 12Cr–1MoVW [57,58] and modified 9Cr–1MoVNb [57] irradiated in FFTF. When a maximum was observed near 400 °C, it occurred at fluences of 25–30 dpa [54–58].

An explanation for the maximum is that beyond the fluence for saturation, irradiation-enhanced softening proceeds to the point where it offsets some of the hardening. That is, thermal aging causes a reduction of strength due to precipitate coarsening

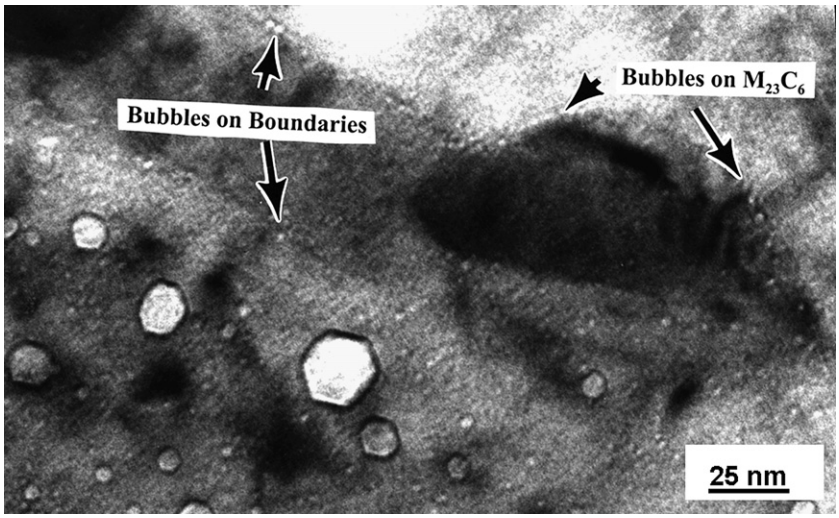

Fig. 4. Bubbles on martensite lath boundaries and on $M_{23}C_6$ precipitates in 9Cr–1MoVW–2Ni steel irradiated in HFIR to ≈75 dpa (760 appm He) at 400 °C [53].

and dislocation recovery [56]. In the absence of irradiation, such softening would occur at 400 °C only after much longer thermal-aging times. Irradiation-enhanced diffusion accelerates the process to produce the maximum in strength. Therefore, the much larger shift in DBTT for a smaller shift in yield stress for steels irradiated to 40 dpa relative to the more recent tests can be explained. With less hardening, the only way to cause a larger shift in DBTT is for there to be a decrease in fracture stress caused by helium (Farrell's third mechanism [47]), as proposed previously [5,6].

This hypothesis can be applied to the latest results on the nickel-doped steels [1]. The lower fluence (12 dpa vs. 40 dpa for the previous work) means that less helium reaches boundaries that are potential sites for fracture initiation than in the 40 dpa tests. Therefore, the helium effect would be expected to be less for the 12 dpa specimens than for 40 dpa specimens, as has been observed. In this case embrittlement is aided by excess hardening by Farrell's first mechanism [47]. Lower helium plus lower irradiation-enhanced diffusion rates at 300 °C provide reasons to expect even less of an effect at this and lower temperatures for the conditions of the recent and previous tests. Because of diffusion, the postulated mechanism would require less helium to produce complete intergranular fracture as the irradiation temperature increases. Furthermore, there appears to be a relationship between the ΔDBTT and helium concentration at 400 °C [1], further enhancing this hypothesis.

Helium generated from boron [8,9,29–33] appears to have a larger effect per amount of helium than helium formed in nickel-doped steels [1,5,6]. Boron can segregate to prior-austenite grain boundaries during austenitization [59–62]. This is a non-equilibrium process, and the amount of segregated boron at prior austenite grain boundaries depends on cooling rate from the austenitization temperature [62]. In recent work to understand stabilization of $M_{23}C_6$ during creep of two 9Cr–W steels, it was determined that boron is incorporated in the $M_{23}C_6$ precipitate to form $M_{23}(C,B)_6$ [63,64]. This occurs during tempering, and the amount of boron in the $M_{23}C_6$ depends on the tempering temperature, time, and the boron composition. For the irradiation studies on boron-containing steels, it is expected the boron will be situated in $M_{23}(C,B)_6$, which is mainly at prior-austenite grain boundaries and lath boundaries. If, as hypothesized above, helium-containing cavities at boundaries act as crack-nucleation sites, then, in boron-doped steels, cavities should form at a lower total helium concentration, since helium from boron forms in the vicinity of the boundaries where fracture is nucleated, thus decreasing the diffusion distance.

Although there was much more helium in the steels irradiated in SINQ [18–22] and the helium-implantation studies than the nickel- and boron-doped steels, the results demonstrated that helium caused intergranular failure [12–14,21,22]. Because of the high helium concentrations in those cases, completely intergranular fractures would be expected

from the above hypothesis. That is what was observed, compared to an ≈75% intergranular fracture surface on a 12Cr–1MoVW–2Ni steel irradiated to 74 dpa and 760 appm He [5]. Henry et al. reached a similar conclusion to that reached from the irradiated nicked-doped steels [5,6] to explain their intergranular failures when they postulated that helium caused a decrease in the critical stress for intergranular fracture [13].

Odette et al. [65] recently proposed a mechanism to explain helium effects similar to that proposed previously [5,6] and discussed here. They posit critical fracture stresses for transgranular cleavage (TGC), σ_c^*, and intergranular fracture (IGF), σ_{ig}^*; brittle fracture for either mode occurs when the critical stress is exceeded in front of a notch or crack tip. According to this formalism, '... gradual weakening of the PAGs [prior-austenite grain boundaries] by helium (and/or other mechanisms) would not be reflected in IGF until σ_{ig}^* falls below σ_c^* ...'. However, the authors acknowledge that such an abrupt change would not be expected and, in reality, a gradual change from TGC to IGF would be expected [65], as was hypothesized previously [6].

4.2. Observations and future experiments

If the above interpretation of the nickel-doped results and other helium-effects studies is correct, then a large effect of helium on impact properties of high-temperature steels may occur for operating conditions in the first wall of a fusion reactor. Since ferritic/martensitic steels are currently the only viable structural material for this application, the need to understand helium effects is of utmost importance. These observations underscore the need for an intense 14 MeV neutron source, so the effect can be studied under conditions applicable to a fusion reactor first wall.

Since an intense 14 MeV neutron source is not on the near-term horizon, simulation experiments and the use of spallation neutron sources must continue to be applied to the problem. Results from the 12 dpa experiment [1] indicate nickel-doping has limitations for relatively low-dose, low-temperature irradiations, since relatively small effects are observed. Likewise, well-known problems are inherent in boron-doping experiments – surface segregation and the production of lithium in concert with helium. Nevertheless, properly planned experiments using nickel and boron isotopes should be possible to elucidate the problem.

Until now, most helium-effects studies have been restricted to temperatures below about 425 °C, since irradiation hardening from displacement damage does not occur in ferritic/martensitic steels at $\gtrsim$425 °C. However, as pointed out previously [6], if the proposed mechanism for the effect of helium on fracture is correct, then under irradiation conditions where high helium concentrations form, much larger bubbles will form at boundaries in shorter times at higher irradiation temperatures.

Such bubble formation on boundaries has been observed in irradiation of nickel-doped steels irradiated in HFIR at 600 °C to ≈40 dpa and ≈400 appm He (Fig. 5) [53]. In this case, relatively large bubbles formed on lath boundaries, but their numbers and

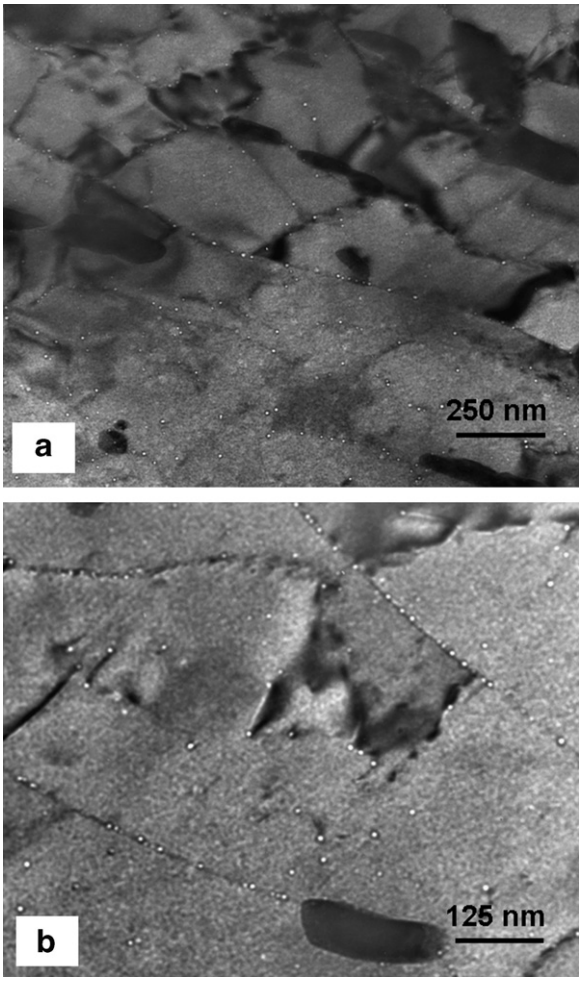

Fig. 5. Bubbles in 12Cr–1MoVW–2Ni steel irradiated in HFIR at 600 °C to ≈40 dpa (a) at low magnification and (b) higher magnification to demonstrate the bubbles on martensite lath boundaries, precipitate boundaries, and in the matrix.

the amount of boundary area covered were much less than observed for the same steel irradiated at 400 °C (Fig. 4). This difference probably results from the change in bubble-nucleation kinetics with increasing temperature. The presence of fewer bubbles plus the absence of radiation hardening at higher temperatures might mitigate against embrittlement. However, the presence of bubbles on a boundary implies the presence of atomic helium on the boundary. Therefore, if helium lowers the resistance to crack propagation, then embrittlement may occur in the absence of any irradiation hardening, meaning the effect could appear above the temperature where irradiation hardening ceases. At the higher temperatures, this is essentially classical elevated-temperature helium embrittlement. Creep and tensile tests at 600 and 700 °C have shown that the ferritic/martensitic steels are relatively immune to this phenomenon [66], although no impact tests have been conducted.

5. Summary and conclusions

Based on nickel-doping studies along with results from studies using boron doping, helium implantation, and spallation neutron source techniques, it was concluded that helium plays a significant role in the hardening and embrittlement after irradiation at temperatures where irradiation hardening occurs (425–450 °C). For low helium concentrations, hardening due to helium occurs over and above hardening due to displacement damage and irradiation-induced precipitation. The increased hardening due to helium causes further embrittlement as determined in an impact test. Helium is probably associated with a higher number density of irradiation-induced defects. It can stabilize vacancy clusters that can increase the number of interstitial clusters that eventually grow into dislocations as well as stabilize clusters to higher temperatures. Small bubbles may also contribute to hardening.

With increasing helium concentration, there is a decrease in fracture stress that is associated with a transition to helium-induced intergranular failure on the lower shelf in an impact test. Complete intergranular failure would not be expected until very large helium concentrations (>1000 ppm) are reached. In the transition region between hardening and complete intergranular failure, it was suggested that small helium-filled cavities or bubbles could become nuclei for fracture and/or enhance crack propagation. Alternatively, or in combination with bubbles on the boundaries, helium atoms on the boundaries could promote fracture. Both processes are caused by the diffusion of helium to grain boundaries, subgrain (martensite lath) boundaries, and precipitate/lattice interfaces, where the small helium bubbles can form.

Although the results of a large number of helium-effects studies using simulation techniques indicate a helium effect on embrittlement of ferritic/martensitic steels, all of the techniques have problems associated with interpreting results. There is a critical need for an intense 14 MeV neutron source in which the problems inherent in the simulation techniques are eliminated.

Acknowledgements

For reviewing the manuscript and for helpful discussions of the subject, Drs D.R. Harries, L.K. Mansur, R.G. Stoller, and S.J. Zinkle are gratefully acknowledged. This research was sponsored by the Office of Fusion Energy Sciences, US Department of Energy, under Contract DE-AC05-00OR22725 with U.T.-Battelle, LLC.

References

[1] R.L. Klueh, N. Hashimoto, M.A. Sokolov, K. Shiba, S. Jitsukawa, J. Nucl. Mater., this issue, doi:10.1016/j.jnucmat.2006.05.048.
[2] R.L. Klueh, J.M. Vitek, J. Nucl. Mater. 161 (1989) 13.
[3] R.L. Klueh, J.M. Vitek, J. Nucl. Mater. 150 (1987) 272.
[4] R.L. Klueh, P.J. Maziasz, J. Nucl. Mater. 187 (1992) 43.
[5] R.L. Klueh, D.J. Alexander, J. Nucl. Mater. 187 (1992) 60.
[6] R.L. Klueh, D.J. Alexander, J. Nucl. Mater. 218 (1995) 15.
[7] R.L. Klueh, E.E. Bloom, Nucl. Eng. Design 73 (1982) 101.
[8] K. Shiba, I. Ioka, J.E. Robertson, M. Suzuki, A. Hishinuma, in: Euromat 96: Conference on Materials and Nuclear Power, Institute for Materials, London, 1996, p. 265.
[9] K. Shiba, A. Hishinuma, J. Nucl. Mater. 283–287 (2000) 474.
[10] R. Lindau, A. Möslang, D. Preininger, M. Rieth, H.D. Röhrig, J. Nucl. Mater. 271&272 (1999) 450.
[11] P. Jung, J. Henry, J. Chen, J.-C. Brachet, J. Nucl. Mater. 318 (2003) 241.
[12] J. Henry, M.-H. Mathon, P. Jung, J. Nucl. Mater. 318 (2003) 249.
[13] J. Henry, L. Vincent, X. Averty, B. Marini, P. Jung, J. Nucl. Mater., in press.
[14] J. Henry, L. Vincent, X. Averty, B. Marini, P. Jung, J. Nucl. Mater., to be published.
[15] L.K. Mansur, A.F. Rowcliffe, M.L. Grossbeck, R.E. Stoller, J. Nucl. Mater. 139 (1986) 228.
[16] G.R. Odette, J. Nucl. Mater. 141–143 (1986) 1057.
[17] L.K. Mansur, W.A. Coghlan, in: N.J. Packan, R.E. Stoller, A.S. Kumar (Eds.), Effects of Irradiation on Materials: 14th International Symposium, ASTM STP 1046, 1, American Society for Testing and Materials, Philadelphia, 1989, p. 315.

[18] X. Jia, Y. Dia, M. Victoria, J. Nucl. Mater. 305 (2002) 1.
[19] Y. Dai, X. Jia, K. Ferrell, J. Nucl. Mater. 318 (2002) 192.
[20] X. Jai, Y. Dia, J. Nucl. Mater. 323 (2003) 360.
[21] Y. Dia, X. Jai, in: Proceedings of Conference on Accelerator Applications in a Nuclear Renaissance, American Nuclear Society, La Grange Park, IL, 2004, p. 857.
[22] Y. Dia, X. Jai, R. Thermer, F. Groeschel, Irradiation Effects in Martensitic Steels Under Neutron and Proton Mixed Spectrum, TM-34-04-08, Paul Scherrer Institut, October 15, 2004.
[23] S.A. Maloy, T. Romero, M.R. James, Y. Dai, J. Nucl. Mater., in press.
[24] K. Farrell, T.S. Byun, J. Nucl. Mater. 296 (2001) 129.
[25] K. Farrell, T.S. Byun, J. Nucl. Mater. 318 (2003) 274.
[26] L.R. Greenwood, J. Nucl. Mater. 115 (1983) 137.
[27] R. Kasada, A. Kimura, H. Matsui, M. Narui, J. Nucl. Mater. 258–263 (1998) 1199.
[28] R. Kasada, A. Kimura, Mater. Trans. 46 (2005) 475.
[29] E.V. van Osch, M.G. Horsten, G.E. Lucas, G.R. Odette, in: M.L. Hamilton, A.S. Kumar, S.T. Rosinski, M.L. Grossbeck (Eds.), Effects of Irradiation on Materials: 19th International Symposium, ASTM STP 1366, American Society for Testing and Materials, West Conshohocken, PA, 2000, p. 612.
[30] M. Rieth, B. Dafferner, H.D. Röhrig, J. Nucl. Mater. 258–263 (1998) 1147.
[31] E.I. Materna-Morris, M. Rieth, K. Ehrlich, in: M.L. Hamilton, A.S. Kumar, S.T. Rosinski, M.L. Grossbeck (Eds.), Effects of Irradiation on Materials: 19th International Symposium, ASTM STP 1366, American Society for Testing and Materials, West Conshohocken, PA, 2000, p. 597.
[32] H.-C. Schneider, B. Dafferner, J. Aktaa, J. Nucl. Mater. 295 (2001) 16.
[33] H.-C. Schneider, B. Dafferner, J. Aktaa, J. Nucl. Mater. 321 (2003) 135.
[34] L.R. Greenwood, J. ASTM Int. 3 (2006).
[35] K. Farrell, J.T. Houston, A. Wolfenden, R.T. King, A. Jostons, in: J.W. Corbett, L.C. Ianniello (Eds.), Radiation-Induced Voids in Metals, CONF-710601, US Atomic Energy Commission, 1972, p. 376.
[36] D.S. Gelles, F.A. Garner, J. Nucl. Mater. 85&86 (1979) 689.
[37] P.J. Maziasz, R.L. Klueh, J.M. Vitek, J. Nucl. Mater. 141–143 (1986) 929.
[38] P.J. Maziasz, R.L. Klueh, in: N.H. Packan, R.E. Stoller, A.S. Kumar (Eds.), Effects of Radiation on Materials: 14th International Symposium, ASTM STP 956, I, American Society for Testing Materials, Philadelphia, 1987, p. 35.
[39] R.L. Klueh, J.M. Vitek, W.R. Corwin, D.J. Alexander, J. Nucl. Mater. 155–157 (1988) 973.
[40] W.L. Hu, D.S. Gelles, in: F.A. Garner, C.H. HenagerJr., N. Igata (Eds.), Influence of Radiation on Material Properties: 13th International Symposium (Part II), ASTM STP 956, American Society for Testing Materials, Philadelphia, 1987, p. 83.
[41] E. Wakai, N. Hashimoto, Y. Miwa, J.P. Robertson, R.L. Klueh, K. Shiba, S. Jitsukawa, J. Nucl. Mater. 283–287 (2000) 334.
[42] J.C. Brachet, X. Averty, P. Lamagnère, A. Alamo, F. Rosenblum, O. Raquet, J.L. Bertin, in: S.T. Rosinski, M.L. Grossbeck, T.R. Allen, A.S. Kumar (Eds.), Effects of Irradiation on Materials: 20th International Symposium, ASTM STP 1405, American Society for Testing and Materials, West Conshohocken, PA, 2002, p. 500.
[43] J. Henry, X. Averty, Y. Dia, P. Lamagnère, J.P. Pizzanelli, J.J. Espinas, P. Wident, J. Nucl. Mater. 318 (2003) 215.
[44] Y. Dia, Y. Foucher, M. James, B. Oliver, J. Nucl. Mater. 318 (2003) 167.
[45] H. Ogiwara, A. Kohyama, H. Tanigawa, H. Sakasegawa, J. Nucl. Mater., to be published.
[46] N. Hashimoto, R.L. Klueh, J. Nucl. Mater. 305 (2002) 153.
[47] K. Farrell, Radiat. Eff. 53 (1980) 175.
[48] J. Hunn, E. Lee, T. Byun, L. Mansur, J. Nucl. Mater. 282 (2000) 131.
[49] Y. Osetsky, D. Bacon, V. Mohles, Phil. Mag. 83 (2003) 3623.
[50] B. Wirth, G. Odette, J. Marian, L. Ventelon, J. Young-Vandersall, L. Zepeda-Ruiz, J. Nucl. Mater. 329–333 (2004) 103.
[51] R.W. Hertzberg, Deformation and Fracture Mechanics of Engineering Materials, third ed., Wiley, New York, 1989, p. 253.
[52] C.J. McMahon Jr., in: L.J. Bonis, J.J. Duga, J.J. Gilman (Eds.), Fundamental Phenomena in the Materials Sciences, vol. 4, Plenum, New York, 1967, p. 247.
[53] P.J. Maziasz, Unpublished research.
[54] A. Kohyama, A. Hishinuma, D.S. Gelles, R.L. Klueh, W. Dietz, K. Ehrlich, J. Nucl. Mater. 233–237 (1996) 138.
[55] K. Shiba, M. Suzuki, A. Hishinuma, J.E. Pawel, in: D.S. Gelles, R.K. Nanstad, A.S. Kumar, E.A. Little (Eds.), Effects of Radiation on Materials: 17th International Symposium, ASTM STP 1270, American Society for Testing and Materials, Philadelphia, 1996, p. 753.
[56] V.S. Khabarov, A.M. Dvoriashin, S.I. Porollo, J. Nucl. Mater. 233–237 (1996) 236;
N.H. Packen, R.E. Stoller, A.S. Kumar (Eds.), Symposium, ASTM STP 1046, American Society for Testing and Materials, Philadelphia, 1990, p. 35.
[57] S.A. Maloy, M.B. Toloczko, K.J. McClellan, T. Romero, Y. Kohno, F.A. Garner, R.J. Kurtz, A. Kimura, J. Nucl. Mater., submitted for publication.
[58] R.L. Klueh, D.J. Alexander, J. Nucl. Mater. 258–263 (1998) 1269.
[59] W.C. Leslie, The Physical Metallurgy of Steels, McGraw-Hill Book Company, New York, 1981, p. 269.
[60] F.B. Pickering, Physical Metallurgy and the Design of Steels, Applied Science Publishers Ltd, London, 1978, p. 103.
[61] T.M. Williams, A.M. Stoneham, D.R. Harries, Met. Sci. 10 (1976) 14.
[62] D.R. Harries, A.D. Marwick, Phil. Trans. Roy. Soc. London A295 (1980) 197.
[63] A. Golpayegani, M. Hättestrand, H.-O. Andrén, in: A. Strang, R.D. Conroy, W.M. Banks, M. Blackler, J. Leggett, G.M. McColvin, S. Simpson, M. Smith, F. Starr, R.W. Vanstone (Eds.), Parsons 2003: Engineering Issues in Turbine Machinery, Power Plant and Renewables, The Institute of Materials, Minerals and Mining, London, 2003, p. 347.
[64] A. Czyrska-Filemonowicz, K. Bryla, K. Spiradek-Hahn, K. Bryla, H. Firganek, A. Zielinska-Lipiec, P.J. Ennis, in: R. Viswanathan, D. Gandy, K. Coleman (Eds.), Advances in Materials Technology for Fossil Power Plants, ASM International, Materials Park, OH, 2005, p. 365.

[65] G.R. Odette, T. Yamamoto, H. Kishimoto, Fusion Mater. Semiann. Prog. Rept. for Period Ending December 31, 2003, DOE/ER-313/35, Department of Energy, April 2004, p. 90.
[66] R.L. Klueh, D.R. Harries, High-Chromium Ferritic and Martensitic Steels for Nuclear Applications, ASTM, West Conshohocken, PA, 2001, p. 135.

Further reading

[1] K. Farrell, P.J. Maziasz, E.H. Lee, L.K. Mansur, Radiat. Eff. 78 (1983) 277.